Magnetism of iron above the Curie temperature

1983 J. Phys. F: Met. Phys. 13 145

(http://iopscience.iop.org/0305-4608/13/1/018)

J. Phys. F: Met. Phys. **13** (1983) 145–160. Printed in Great Britain

Magnetism of iron above the Curie temperature

Tamio Oguchi, Kiyoyuki Terakura and Noriaki Hamada

Institute for Solid State Physics, University of Tokyo, Roppongi, Minatoku, Tokyo 106, Japan

Received 15 June 1982

Abstract. The electronic structure of paramagnetic iron is calculated self-consistently within the local spin density functional formalism by applying the coherent potential approximation with the muffin-tin potential model. The effective exchange parameters J_n are calculated as the interaction energy between two magnetic moments in the paramagnetic medium obtained. A discussion on the magnetism of iron above the Curie temperature is presented using the Heisenberg model with the calculated J_n.

1. Introduction

The itinerant magnetism of the transition metals, their compounds and alloys can be described quantitatively by band theory (Stoner theory) with the use of the local spin density functional (LSDF) formalism (von Barth and Hedin 1972, Gunnarsson and Lundqvist 1976) as far as the ground state is concerned (see, e.g., Callaway and Wang 1977, Moruzzi *et al* 1978). On the other hand, the magnetism at finite temperatures cannot be described even qualitatively by Stoner theory and has been one of the most difficult subjects in theoretical solid state physics.

Several theoretical works making use of the functional integral method (Moriya and Takahashi 1978, Hubbard 1979a, b, 1981, Prange and Korenman 1979a, b, Hasegawa 1979, 1980) have recently brought considerable progress to this field and several thermodynamic quantities of iron and nickel, in particular the magnetisation curve as a function of temperature, the Curie temperature and the Curie–Weiss susceptibility law, have been reproduced qualitatively. However, most of the works are based on the simplified model Hamiltonian, mainly the single-band Hubbard model, and it is highly desirable to incorporate realistic one-electron states into the theory. This will make the quantitative comparison between theory and experiment meaningful and clarify the consequences of other approximations in the theory.

This paper is the first step of our continuing work in this direction and deals with the magnetic properties of iron above T_C. Firstly, we assume that the direction of the local magnetic moments is random, which means we neglect short-range magnetic order (SRMO). By regarding the system as an alloy, the electronic structure is calculated self-consistently by using the coherent potential approximation (CPA) and the LSDF formalism. We find from this calculation that the magnitude of the local moment in the paramagnetic state is only slightly reduced compared with that in the ground state. Secondly, the effective exchange parameters J_n are evaluated as the interaction energy between two magnetic moments in the calculated effective paramagnetic medium. A characteristic

0305-4608/83/010145 + 16$02.25

feature of our J_n is that the first nearest-neighbour interaction J_1 is strongly ferromagnetic and the magnitude of J_n drops off very rapidly for the further neighbours. Such a rapid drop is not seen in J_n in other works (Lin-Chung and Holden 1981, Holden and You 1982, Wang *et al* 1982). In particular, the result of Wang *et al* is very different from ours. A brief discussion will be given on this point. Finally, a discussion of the magnetic properties of iron above T_C is presented using the Heisenberg model with the exchange parameters obtained. We estimate the Curie temperature T_C by the Green function method and obtain $T_C = 2700$ K. (Note that the quantum correction is included in the calculation of T_C.) The SRMO calculated in this way turns out to be fairly small; this is consistent with the initial assumption. We also calculate the neutron scattering function $S(\boldsymbol{q}, \omega)$ with the three-pole approximation of Lovesey and Meserve (1973) and compare the results with the experiment of Lynn (1975).

2. Formalism

2.1. Modelling of the paramagnetic state

For iron above the Curie temperature, we consider a system in which the magnetic moments of all iron atoms have the same magnitude but are directed randomly. This corresponds to the neglect of SRMO, in contrast to the assumption of Wang *et al* (1982). Regarding this system as an alloy and applying CPA with the muffin-tin model (Gyorffy and Stocks 1979), we calculate the electronic band structure self-consistently within the LSDF formalism (Gunnarsson and Lundqvist 1976). The present calculation corresponds to the local saddle-point approximation (Hasegawa 1979) in the functional integral method. The local saddle-point approximation may work well for iron because the magnetic moment of iron has a localised character and its longitudinal fluctuation is relatively small.

2.2. Muffin-tin CPA for the system with random spin direction

The one-electron potential for the system is written in the muffin-tin form as

$$\mathbf{V}(\boldsymbol{r}) = \sum_n \mathbf{v}_n(|\boldsymbol{r} - \boldsymbol{R}_n|) \tag{1}$$

where $\boldsymbol{R}_n$ is the position vector of the atom n. As the magnetic moments have random orientation, $\mathbf{v}_n$ is a matrix in the spin space expressed as

$$\mathbf{v}_n(r) = \tfrac{1}{2}(v_+(r) + v_-(r))\begin{pmatrix} 1 & 0 \\ 0 & 1 \end{pmatrix} + \tfrac{1}{2}(v_+(r) - v_-(r))\begin{pmatrix} \cos\theta_n & \exp(-i\varphi_n)\sin\theta_n \\ \exp(i\varphi_n)\sin\theta_n & -\cos\theta_n \end{pmatrix} \tag{2}$$

where θ_n and φ_n specify the direction of the magnetic moment of the nth atom and v_+ (v_-) is the potential seen by an electron whose spin is parallel (antiparallel) to the spin quantisation direction at a site. Equation (2) is rewritten as

$$\mathbf{v}_n(r) = \tfrac{1}{2}(v_+(r) + v_-(r))\mathbf{I} + \tfrac{1}{2}(v_+(r) - v_-(r))(\boldsymbol{e}_n \cdot \boldsymbol{\sigma}) \tag{3}$$

where $\mathbf{I}$ is the 2×2 unit matrix, $\boldsymbol{e}_n$ is a unit vector in the direction of the spin quantisation axis at the site n and $\boldsymbol{\sigma}$ is a vector spanned by the Pauli matrices, σ_x, σ_y and σ_z. The single-site t matrix is also expressed as

$$\mathbf{t}_n = \tfrac{1}{2}(\bar{t}_+ + \bar{t}_-) \times \mathbf{I} + \tfrac{1}{2}(\bar{t}_+ - \bar{t}_-) \times (\boldsymbol{e}_n \cdot \boldsymbol{\sigma}) \tag{4}$$

where $\bar{t}_+$ ($\bar{t}_-$) is a matrix whose columns and rows are specified by the orbital angular momenta and its matrix element is given by

$$(\bar{t}_\alpha)_{LL'} = -\kappa^{-1} \sin \delta_l^\alpha \exp(\mathrm{i}\delta_l^\alpha)\delta_{LL'} \qquad \alpha = + \text{ or } - \tag{5}$$

with δ_l^α the phase shift of the lth partial wave. In equation (4), the multiplication sign is the direct product of the matrices.

The scattering path operator $\boldsymbol{\tau}$ is formally expressed in the same way as usual (Gyorffy and Stocks 1979):

$$\boldsymbol{\tau} = (\mathbf{t}^{-1} - \mathbf{G})^{-1} \tag{6}$$

where $\mathbf{t}$ is site diagonal and its diagonal block of the site n is given by equation (4). $\mathbf{G}$ is given by

$$\mathbf{G} = \bar{G} \times \mathbf{I} \tag{7}$$

with $\bar{G}$ the structure Green function in the usual KKR formalism. So far the quantity $\bar{Q}$ denotes a matrix in the site and the orbital angular momentum space but we write it as Q hereafter to simplify the notation.

By applying CPA, a coherent single-site t matrix $\mathbf{t}_c$ is determined by

$$\int \mathrm{d}\Omega \, \mathbf{K}(\boldsymbol{e}_0) = 0 \tag{8}$$

where $\int \mathrm{d}\Omega$ means an integration over the angle $\boldsymbol{e}_0$ and

$$\mathbf{K}(\boldsymbol{e}_0) = (1 - \delta\mathbf{t}^{-1}\boldsymbol{\tau}^c)^{-1}\delta\mathbf{t}^{-1} \tag{9}$$

with

$$\delta\mathbf{t}^{-1} = (\mathbf{t}_c^{-1} - \mathbf{t}_0^{-1})\delta_{n0}\delta_{n'0}. \tag{10}$$

$\mathbf{t}_0$ is given by equation (4) with $n = 0$. $\boldsymbol{\tau}^c$ in equation (9) is the scattering path operator for the ordered effective medium consisting of only the coherent t matrix $\mathbf{t}_c$ at each site. As we are dealing with the paramagnetic state, the system has spherical symmetry in the spin space so that $\mathbf{t}_c$ has the form

$$\mathbf{t}_c = t_c \times \mathbf{I}. \tag{11}$$

Inserting equations (7) and (11) into equation (6), we obtain

$$\boldsymbol{\tau}^c = \tau^c \times \mathbf{I} \tag{12}$$

with

$$(\tau^c)^{nn'}_{LL'} = \left(\sum_{\boldsymbol{k}} (t_c^{-1} - G(\boldsymbol{k}))^{-1} \exp[\mathrm{i}\boldsymbol{k} \cdot (\boldsymbol{R}_n - \boldsymbol{R}_{n'})] \right)_{LL'}. \tag{13}$$

The averaged integrated density of states per spin is calculated in terms of the coherent t matrix by (Gyorffy and Stocks 1979)

$$N(\varepsilon) = N_0(\varepsilon) - \frac{1}{\pi} \operatorname{Im} \ln \det(t_c^{-1} - G) - \frac{1}{8\pi^2} \int \mathrm{d}\Omega \operatorname{Im} \ln \det[1 - (\mathbf{t}_c^{-1} - \mathbf{t}_0^{-1})(\boldsymbol{\tau}^c)^{00}] \tag{14}$$

where $N_0(\varepsilon)$ is the integrated density of states for the free electron. Equation (14) is used to determine the Fermi level. In order to construct the new potentials $v_+(r)$ and $v_-(r)$ with the LSDF formalism (Gunnarsson and Lundqvist 1976), we have to calculate the corresponding electron densities $\rho^+(r)$ and $\rho^-(r)$. This can be done firstly by setting

$\boldsymbol{e}_0=(0,0,1)$ and by using the formula (Gyorffy and Stocks 1979)

$$\rho^{\alpha}(\boldsymbol{r})=\int_{\cdot}^{\cdot\varepsilon_F} d\varepsilon\left(-\frac{1}{\pi}\right)\sum_{L}|\Delta_L^{\alpha}(\boldsymbol{r};\varepsilon)|^2\ \mathrm{Im}(\tau^{\alpha})_{LL}^{00} \tag{15}$$

with

$$\Delta_L^{\alpha}(\boldsymbol{r};\varepsilon)=-\kappa R_l^{\alpha}(r;\varepsilon)Y_L(\hat{r})/\sin\delta_l^{\alpha} \tag{16}$$

and

$$(\tau^{\alpha})_{LL}^{00}=(\tau^{c})_{LL}^{00}+(\tau^{c})_{LL}^{00}(K^{\alpha})_{LL}(\tau^{c})_{LL}^{00}. \tag{17}$$

$\mathbf{K}(\boldsymbol{e}_0)$ of equation (9) is diagonal in spin space with the choice $\boldsymbol{e}_0=(0,0,1)$ and K^{α} with $\alpha=+$ (or $-$) refers to the up (down) spin block of $\mathbf{K}(\boldsymbol{e}_0)$. δ_l^{α} is the phase shift in equation (5) and $R_l^{\alpha}(r;\varepsilon)$ is the radial wavefunction normalised so that it is equal to $\cos\delta_l^{\alpha}j_l(\kappa r_{MT})-\sin\delta_l^{\alpha}n_l(\kappa r_{MT})$ at the muffin-tin sphere radius r_{MT}. The choice of $\boldsymbol{e}_0$ along the z direction does not violate the generality of the argument, because the effective medium has spherical symmetry in the spin space and all directions of $\boldsymbol{e}_0$ are physically equivalent. However, as we are using the z direction as the global spin quantisation axis, the above choice of $\boldsymbol{e}_0$ is most convenient from the practical point of view.

Before ending this subsection, we make an important comment on the consequence of equation (8). We can rewrite equation (9) as

$$\mathbf{K}(\boldsymbol{e}_0)=\tfrac{1}{2}(K^{+}+K^{-})\times\mathbf{I}+\tfrac{1}{2}(K^{+}-K^{-})\times(\boldsymbol{e}_0\cdot\boldsymbol{\sigma}). \tag{18}$$

Therefore, equation (8) is reduced to

$$K^{+}+K^{-}=0 \tag{19}$$

which is equivalent to the CPA condition for the system where only the up and down spin configurations occur with an equal probability. Similarly, we can replace the last contribution in equation (14) with

$$-\frac{1}{2\pi}\sum_{\alpha=+,-}\mathrm{Im}\ln\det[1-(t_c^{-1}-t_{\alpha}^{-1})(\tau^{c})^{00}]. \tag{20}$$

2.3. Calculation of the effective exchange parameters

We specify two magnetic moments at the origin and $\boldsymbol{R}_n$ in the effective medium obtained by the muffin-tin CPA calculation and consider two cases where these two moments are parallel (P) and antiparallel (AP). The interaction energy between the two moments is evaluated by

$$\Delta E_{P(AP)}=\frac{2}{\pi}\int_{\cdot}^{\cdot\varepsilon_F} d\varepsilon\ \mathrm{Im}\ln\det(1-(+)K^{\alpha}(\tau^{c})^{0n}K^{\alpha}(\tau^{c})^{n0}) \tag{21}$$

where α can take both $+$ and $-$ signs because of equation (19). A derivation of equation (21) is presented in appendix 1. The effective exchange parameter J_n is defined as the difference between the interaction energies of the parallel and antiparallel moments:

$$J_n=-(\Delta E_P-\Delta E_{AP})/2S^2 \tag{22}$$

where S is the magnitude of the atomic spin. Equation (22) is equivalent to that derived by Inoue and Moriya (1967) and Lacour-Gayet and Cyrot (1974) in the tight-binding

formalism. We assume the J_n to be the exchange parameters in the Heisenberg model:

$$H = -\sum_{(i,j)} J_{ij} \boldsymbol{S}_i \cdot \boldsymbol{S}_j. \tag{23}$$

2.4. Calculation of the thermodynamic properties

Some thermodynamic properties for paramagnetic iron are evaluated within the framework of the spherical model as in the work of Shastry *et al* (1981). The spin correlation function is written as

$$\langle S^z(\boldsymbol{q}) S^z(-\boldsymbol{q}) \rangle = k_B T (J(0) - J(\boldsymbol{q}) + \lambda) \tag{24}$$

where

$$J(\boldsymbol{q}) = \sum_n J_n \exp(\mathrm{i}\boldsymbol{q} \cdot \boldsymbol{R}_n) \tag{25}$$

and the inverse susceptibility λ is determined by the sum rule

$$\tfrac{1}{3} S(S+1) = \frac{1}{N} \sum_{\boldsymbol{q}} \langle S^z(\boldsymbol{q}) S^z(-\boldsymbol{q}) \rangle. \tag{26}$$

The correlation function between the two spins separated by $\boldsymbol{R}_n$ is given by

$$\langle S_0^z S_n^z \rangle = \frac{1}{N} \sum_{\boldsymbol{q}} \langle S^z(\boldsymbol{q}) S^z(-\boldsymbol{q}) \rangle \exp(-\mathrm{i}\boldsymbol{q} \cdot \boldsymbol{R}_n). \tag{27}$$

The Curie temperature is obtained as the temperature at which $\lambda = 0$ in equations (24) and (26).

In order to calculate the neutron scattering function $S(\boldsymbol{q}, \omega)$ we use the three-pole approximation of Lovesey and Meserve (1973) for the relaxation shape function $F(\boldsymbol{q}, \omega)$. This part of the calculation is also parallel to that of Shastry *et al* (1981). In appendix 2, a short comment is given on the evaluation of the fourth moment of $F(\boldsymbol{q}, \omega)$.

3. Results and discussions

3.1. Band structure

The local density of states (DOS) for iron in the paramagnetic state is shown in figure 1. The special direction method of Bansil (1975) is adopted to evaluate the $\boldsymbol{k}$ space summation in equation (13). Good accuracy is obtained with a total of 500 points in $\frac{1}{48}$th of the Brillouin zone (5 special directions and 100 uniform meshes along each direction), because the spectral function at each $\boldsymbol{k}$ point has an appreciable width due to the randomness in the system. Compared with the ferromagnetic DOS (Callaway and Wang 1977, Moruzzi *et al* 1978), the broadening of the paramagnetic band is due to the mixing of the up and down spin states caused by the randomness in the direction of the magnetic moment. Although the present DOS has much sharper structures, the general features are similar to that of Hasegawa (1979). The experimental DOS for ferromagnetic and paramagnetic iron were given by Petersson *et al* (1976) using photoelectron spectroscopy. They concluded that there were no substantial changes in the DOS due to a change in the magnetic configuration. However, figure 7 in their paper does show that the peak at 3 eV below the

Fermi energy becomes prominent at T_c. This tendency is consistent with the present DOS in figure 1.

The magnitude of the magnetic moment in the muffin-tin sphere is $2.17\mu_B$. We used 2.89 Å as the lattice constant, taking account of a lattice expansion (1% of the value at 0 °C) due to temperature (Nix and MacNair 1941). For ferromagnetic iron with the same lattice constant, we have obtained a magnitude of $2.29\mu_B$ using the KKR band calculation. This implies that the magnitude of the magnetic moment hardly changes under the transition from the ferromagnetic to the paramagnetic configuration and reminds us of the fact that the magnetic moment of iron has a strong self-maintaining character. The change in moment in the muffin-tin sphere, taking the Fermi distribution function in equation (15) into account, is rather small ($-0.02\mu_B$). If we estimate the change in the potential due to the above effect from $\Delta v = \Delta m I$ with $I \sim 0.1$ Ryd for iron, we get, at most, some mRyd. Therefore, the neglect of the temperature dependence through the Fermi distribution function is a reasonable approximation for $T \sim 1000$ K.

3.2. Effective exchange parameters

The effective exchange parameters J_n for paramagnetic iron are shown in table 1 together with those calculated for two magnetic moments in a non-magnetic iron host. Note that we assumed $S = 1$ in equation (22). In the case of the non-magnetic host, we use equations (A.21) and (A.23) instead of equation (21) as the interaction energy between the two magnetic moments, because there is no condition corresponding to equation (19). The most remarkable characteristic in the parameters for paramagnetic iron is that the nearest-neighbour coupling J_1 is quite large and the others are negligibly small. It is seen through a comparison with the J_n for the non-magnetic iron case that this characteristic comes from

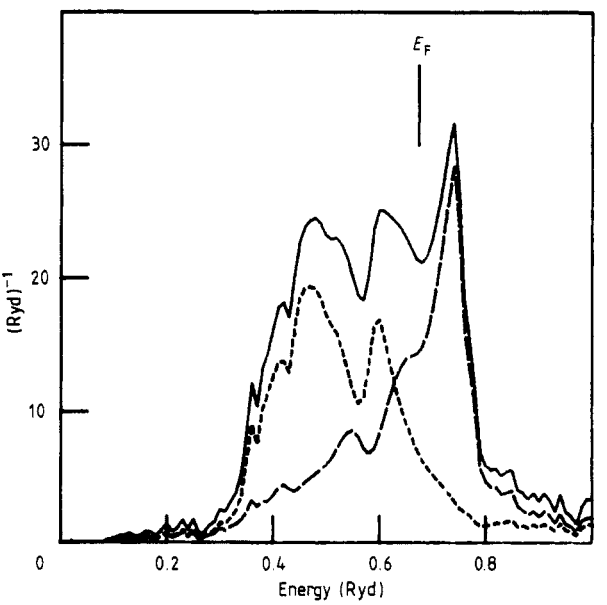

Figure 1. The local DOS for paramagnetic iron. The full, short broken and long broken lines represent the total, majority-spin and minority-spin bands, respectively. The vertical line represents the Fermi energy (0.674 Ryd).

Table 1. The effective exchange parameters J_n for paramagnetic and non-magnetic iron (in meV).

n	Paramagnetic	Non-magnetic
1	54.34	19.94
2	−1.37	−3.90
3	3.25	14.60
4	0.19	−1.80
5	−0.56	−1.54
6	0.51	−0.21
7	−0.25	−0.21

the randomness effect in the direction of the magnetic moments. A similar behaviour was observed in the calculation of the pairwise interactions in the binary transition metal alloys by Bieber *et al* (1981). The second characteristic in our parameters is that J_1 and J_3 are ferromagnetic and J_2 is antiferromagnetic, for both the paramagnetic and non-magnetic iron cases. The signs of the exchange coupling up to the third neighbour are completely parallel to those of the non-local susceptibilities calculated by Terakura *et al* (1982). We therefore believe that the trend seen in the signs of J_n up to $n=3$ in this calculation is a proper characteristic of iron. Comparing the present results with those of other workers (Lin-Chung and Holden 1981, Holden and You 1982, Wang *et al* 1982), we find some qualitative differences. The result of Lin-Chung and Holden (1981) seems to be the closest to ours in the sense that their J_1 is comparable with our J_1 and somewhat larger than the other J_n in magnitude. However, their J_5 is about −20 meV, which is quite different from our J_5 (−0.56 meV). The results of Wang *et al* (1982), which are based on the assumption of a large SRMO, show quite different features from ours. Their J_n remain appreciable over a very long range and J_2 is strongly ferromagnetic. We should note that Wang *et al* (1982) started from an opposite extreme to us. It is hard to believe that the simple Heisenberg model works for all the magnetic configurations of iron and, in fact, the work of the Cambridge group (You and Heine 1982, Holden and You 1982) indicates that the Heisenberg model is meaningful within limited configurations. This may in turn support the use of the Heisenberg model if the temperature range is limited and the exchange parameters are estimated using the configuration which is most probable in this temperature range. We calculated J_n by assuming that the paramagnetic state of iron has a small SRMO and, as will be shown in the next subsection, the SRMO estimated using the J_n obtained is small. In this sense, our calculation is consistent. On the other hand, the calculation of Wang *et al* (1982) is not self-consistent, because their J_n calculated by assuming large SRMO do not produce large SRMO. Therefore, at the present stage of approximation, the present J_n seem to be more appropriate for describing the magnetism of iron at high temperatures, although we will also encounter some serious difficulties in the next subsection.

3.3. Thermodynamic properties

The calculated Curie temperature is 2700 K, which is rather higher than the experimental value (1044 K). As mentioned in the previous section, an appreciable reduction of the Curie temperature is not expected from the temperature dependence of the Fermi distribution function. This point does not agree with the calculation of Kakehashi (1981b), in which the Curie temperature decreases by about 30% when the Fermi distribution

function is taken into account. It should also be noted that in most of the estimations of T_C so far, the quantum correction is not included. This means that $S(S+1)$ on the left-hand side of equation (26) is replaced by S^2, which reduces T_C by a factor of two in the case of iron.

The theoretical inverse susceptibility normalised by T_C is shown in figure 2 with the experimental data of Nakagawa (1956). The agreement between the theoretical susceptibility and the experimental one is quite good. Therefore, the Curie–Weiss constant is quite successfully reproduced by our calculation. Our theoretical susceptibility also agrees fairly well with that calculated by Shastry *et al* (1981), although our J_n are quite different from theirs. They calculated the J_n by fitting to the observed spin-wave dispersion at room temperature with some constraints.

Figure 3(*a*) shows the reduced spin correlation function

$$\Gamma(n)=\langle S_0^z S_n^z\rangle/\langle (S_0^z)^2\rangle \tag{28}$$

at $T=1.28T_C$ as a function of the distance between neighbouring iron atoms. Figure 3(*b*) shows the temperature dependence of $\Gamma(n)$ between $T=1.05T_C$ and $1.40T_C$ for $n=1$, 2 and 3. It is clear from these figures that the SRMO is fairly small, which is consistent with our starting assumption. This small SRMO coincides with the results obtained by Hasegawa (1981), Shastry *et al* (1981) and Kakehashi (1981a). Quite recently, Moriya (1982) has investigated the magnetism of typical ferromagnets based on his unified spin fluctuation theory using parameters deduced from the experimental data and found a similar magnitude for the SRMO for iron.

From the equation for the excitation energy of the free magnon

$$\hbar\omega(\boldsymbol{q})=S(J(0)-J(\boldsymbol{q})) \tag{29}$$

the stiffness constant D at low temperature is found to be 550 (meV Å^2), which is very

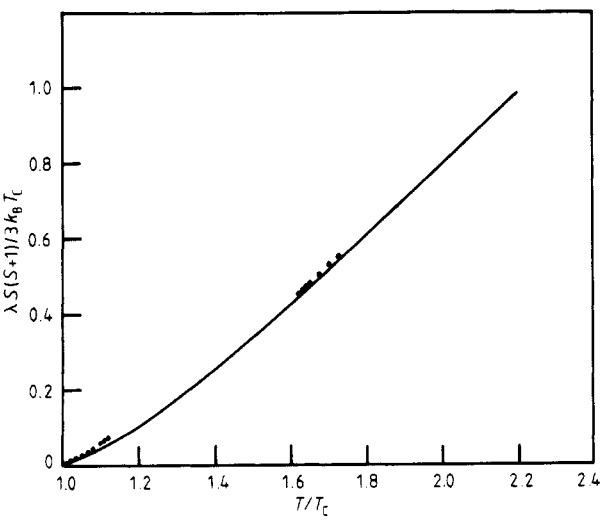

Figure 2. The reduced inverse susceptibility as a function of the reduced temperature T/T_C. The full curve represents the theoretical susceptibility and the full circles represent the experimenta data of Nakagawa (1956).

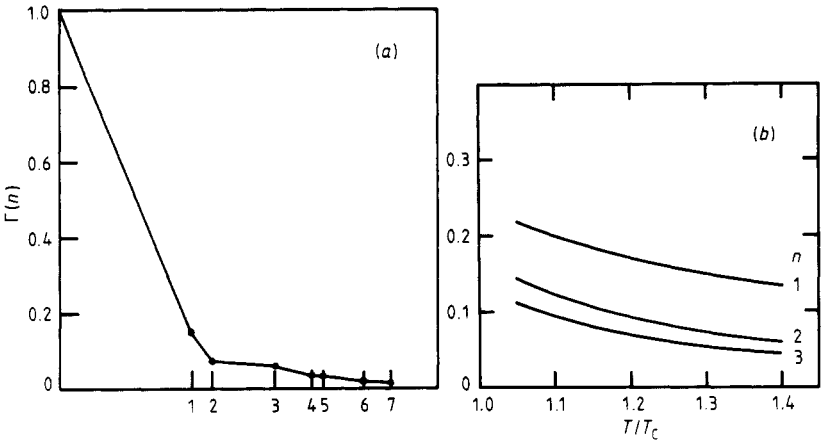

Figure 3. (*a*) The reduced static spin correlation function $\Gamma(n)$ as a function of the distance between the neighbouring iron atoms obtained at $T=1.28T_C$. (*b*) The temperature dependence of the reduced static spin correlation function $\Gamma(n)$ for $n=1$, 2 and 3.

close to the value calculated by Wang *et al* (1982). D obtained in this way does not correspond directly to the spin wave at low temperature because our J_n are calculated for paramagnetic iron. Nevertheless, it gives a reasonable scale qualitatively.

In order to discuss the spin wave above T_C, we calculated the neutron scattering function $S(\boldsymbol{q}, \omega)$ for several temperatures. Figure 4 shows $S(\boldsymbol{q}, \omega)$ for $\boldsymbol{q}$ in the (110) direction at $T=1.28T_C$. It can be seen from this figure that a constant-ω plot of $S(\boldsymbol{q}, \omega)$ for all ω indicates the presence of an apparent peak, whose position agrees well with the spin-wave dispersion observed by Lynn (1975), though its width is broadened. Figure 5(*a*) shows experimental and theoretical dispersion curves above T_C in the (110) direction. The agreement is satisfactory. In addition, the two theoretical curves for $T=1.28T_C$ and $1.40T_C$ are essentially the same, which is also consistent with the experimental result that the spin-wave dispersion shows no detectable change from T_C to $1.40T_C$. However, the peak height of $S(\boldsymbol{q}, \omega)$ decreases substantially with temperature, reflecting the temperature dependence of $\Gamma(n)$ in figure 3(*b*). Figure 6 shows our theoretical prediction of this effect for some values of ω. Experimentally (Lynn 1975), the spin-wave intensity with $\hbar\omega=29$ meV decreases by a factor of about 2.1 from just above T_C to $1.40T_C$ and the corresponding theoretical value for $\hbar\omega=30$ meV in figure 6 is about 1.9. Figure 5(*b*) shows theoretical dispersion curves at $T=1.28T_C$ for the three principal $\boldsymbol{q}$ directions. Some appreciable differences can be seen for $q/q_{max} > 0.4$. (Note that q_{max} in figure 5(*b*) is for the (110) direction and the dispersion curves for (100) and (111) are also plotted by using the same q_{max}.)

In contrast to the apparent success in the above constant-ω plot, there is a serious problem in the constant-$\boldsymbol{q}$ plot. Our $S(\boldsymbol{q}, \omega)$ does not show a peak at $\omega \neq 0$ for the constant-$\boldsymbol{q}$ plot for $q < 0.5q_{max}$, implying the absence of the propagating mode, while figure 10 in Lynn (1975) shows an unmistakable peak at $\hbar\omega=20$ meV for $q=0.3q_{max}$, which corresponds to the full curve in figure 5(*a*). However, it may be worthwhile to note that the present $S(\boldsymbol{q}, \omega)$ in the constant-$\boldsymbol{q}$ plot produces peaks at $\omega \neq 0$ near the zone boundary ($q > 0.7q_{max}$), as shown in figure 4.

Anyway, the failure to predict the propagating mode for smaller q values is the most serious shortcoming of the present theory, as in that of Shastry *et al* (1981).

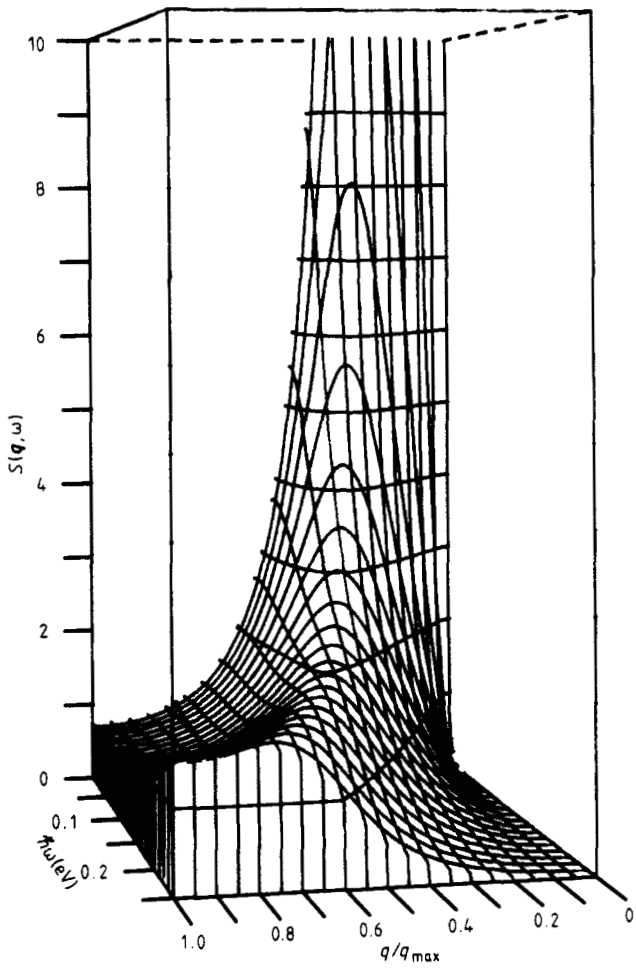

Figure 4. The perspective of the neutron scattering function $S(\boldsymbol{q}, \omega)$ calculated for $\boldsymbol{q}$ in the (110) direction at $T = 1.28T_C$.

4. Concluding remarks

We calculated the electronic structure of paramagnetic iron using the muffin-tin CPA. In the calculation, each iron atom is allowed to have a local magnetic moment with random direction. It was found that the decrease in magnitude of the magnetic moment due to the randomness in its direction is quite small. Our DOS curve for the paramagnetic state is consistent with the photoemission experiment.

The effective exchange parameters J_n were calculated as the interaction energy between the two magnetic moments in the paramagnetic medium obtained. The most remarkable feature of the present J_n is that the first-neighbour coupling J_1 is strongly ferromagnetic and the others are negligibly small compared with J_1. We discussed some qualitative differences between the present J_n and those by other workers (Lin-Chung and Holden 1981, Holden and You 1982, Wang *et al* 1982).

Some thermodynamic properties were then calculated by using the Heisenberg model with the J_n obtained. Our theoretical T_C including the quantum correction is 2700 K,

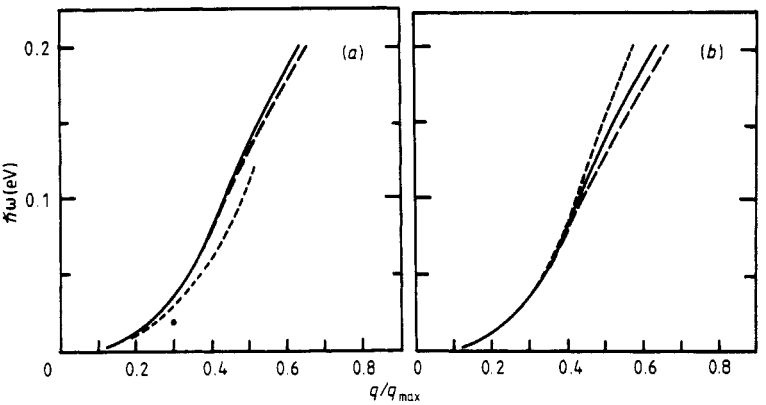

Figure 5. (*a*) The spin-wave dispersion curves along the (110) direction. The full and long broken curves represent the theoretical curves at $T=1.28T_C$ and $1.40T_C$, respectively. The short broken curve and the full circle represent the experimental data above T_C for the constant-ω and constant-$\boldsymbol{q}$ plots respectively, observed by Lynn (1975). (*b*) The theoretical spin-wave dispersion curves along the three principal $\boldsymbol{q}$ directions at $T=1.28T_C$. The full, short broken and long broken curves represent the dispersion curves along the (110), (111) and (100) directions, respectively.

which is too high compared with the experimental value of 1044 K. The short-range magnetic order above T_C was shown to be fairly small and the Curie–Weiss constant was reproduced quite successfully. We have also calculated the neutron scattering function $S(\boldsymbol{q}, \omega)$ in the three-pole approximation. The calculated $S(\boldsymbol{q}, \omega)$ shows an apparent peak in the constant-ω plot and the spin-wave dispersion curve obtained by connecting the peaks is in fairly good agreement with the experimental result of Lynn (1975). However, no definite

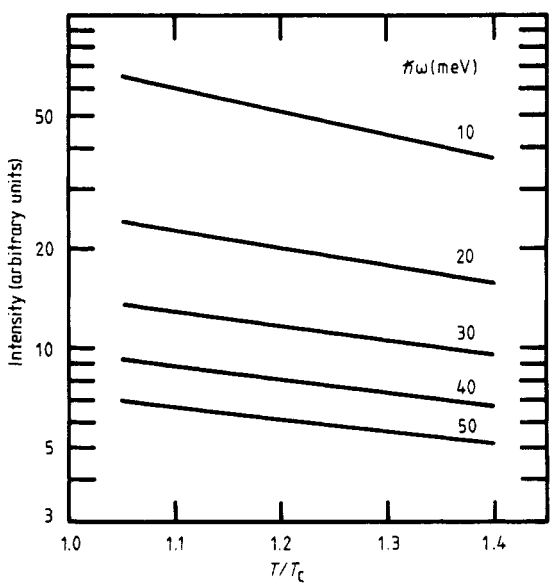

Figure 6. The temperature dependence of the spin-wave intensity for several spin-wave energies.

peak was found for $q < 0.5q_{max}$ in the constant-$\boldsymbol{q}$ plot. This is the most serious qualitative disagreement of the present theory with experiments. No reliable theory is available that can consistently explain the experimental Curie–Weiss constant as well as the persistence of the spin-wave mode up to $1.4T_C$ (see Prange 1981, Edwards 1981).

The present work is the first step in our attempt to understand finite-temperature magnetism on the basis of a realistic electronic structure calculation and several improvements may be conceivable. We are now aiming to proceed along the line of the formalism developed by Moriya and Hasegawa (1980), which gives us a prescription for estimating the pair exchange parameters and the longitudinal fluctuation of the magnetic moment in a self-consistent way.

Acknowledgments

The authors would like to express their sincere thanks to Professor Toru Moriya for helpful discussions. The numerical computation was done by HITAC M-200H at the Computer Center of the Institute for Molecular Science. Some parts of the work were finished while one of the authors (KT) was staying at the IBM Thomas J Watson Research Center under the visiting scientist program. Financial support for the visit from IBM World Trade Corporation is gratefully acknowledged. Thanks are also given to Dr A R Williams for warm hospitality and useful comments. This work was supported in part by a Grant-in-Aid for Cooperative Research from the Ministry of Education, Science and Culture.

Appendix 1. Interaction energy between two impurities

First we derive an expression for the change of the total DOS due to impurities in the muffin-tin model. The derivation is a straightforward extension of the work by Temmerman (1982).

Now, we consider a system in which atoms of M sites with t_n $(n = 1 - M)$ are replaced by impurities with t'_n. By dividing the KKR matrix into the impurity site block and the unperturbed one, the τ matrix for the impurity system is written as

$$\tau^{\mathrm{I}} = \begin{pmatrix} \psi^{I} & -G \\ -\tilde{G} & \theta \end{pmatrix}^{-1} \tag{A.1}$$

where ψ^{I} is the impurity site diagonal block

$$(\psi^{\mathrm{I}})^{nn'}_{LL'} = t'^{-1}_{n,L}\delta_{nn'}\delta_{LL'} - G_{LL'}(\boldsymbol{R}_n - \boldsymbol{R}_{n'}) \tag{A.2}$$

where n and n' refer to the impurity sites, G and $\tilde{G}$ are the off-diagonal blocks consisting only of the structure Green function and θ is the unperturbed site block. For the unperturbed system, the τ matrix is written in a similar form as

$$\tau^{\mathrm{U}} = \begin{pmatrix} \psi^{\mathrm{U}} & -G \\ -\tilde{G} & \theta \end{pmatrix}^{-1}. \tag{A.3}$$

We introduce a Δ matrix as the perturbation due to the impurities:

$$\Delta=(\tau^{\mathrm{U}})^{-1}-(\tau^{\mathrm{I}})^{-1}=\begin{pmatrix}\psi^{\mathrm{U}}-\psi^{\mathrm{I}} & 0\\ 0 & 0\end{pmatrix} \tag{A.4}$$

$$\Delta_{LL'}^{nn'}=\begin{cases}(t_{n,L}^{-1}-t_{n,L}'^{-1})\delta_{nn'}\delta_{LL'} & \text{for } n=1-M\\ 0 & \text{elsewhere.}\end{cases} \tag{A.5}$$

Then τ^{I} is expressed in terms of τ^{U} and Δ:

$$\tau^{\mathrm{I}}=\tau^{\mathrm{U}}+\tau^{\mathrm{U}}\Delta\tau^{\mathrm{I}} \tag{A.6}$$

$$\tau^{\mathrm{I}}=\tau^{\mathrm{U}}(1-\Delta\tau^{\mathrm{U}})^{-1}. \tag{A.7}$$

If we define K by

$$K=(1-\Delta\tau^{\mathrm{U}})^{-1} \tag{A.8}$$

we can also write

$$\tau^{\mathrm{I}}=\tau^{\mathrm{U}}+\tau^{\mathrm{U}}K\tau^{\mathrm{U}}. \tag{A.9}$$

The DOS per spin for the impurity system is given as (Gyorffy and Stocks 1979)

$$n(\varepsilon)=n_0(\varepsilon)-\frac{1}{\pi}\,\mathrm{Im\ Tr}\left(\tau^{\mathrm{I}}\frac{\partial}{\partial\varepsilon}(t'^{-1}-G)\right) \tag{A.10}$$

where $n_0(\varepsilon)$ is the DOS for the free electron and Tr means the trace over all sites and all L. Using equations (A.4) and (A.9), equation (A.10) is rewritten as

$$\begin{aligned}n(\varepsilon)&=n_0(\varepsilon)-\frac{1}{\pi}\,\mathrm{Im\ Tr}\left((\tau^{\mathrm{U}}+\tau^{\mathrm{U}}K\tau^{\mathrm{U}})\frac{\partial}{\partial\varepsilon}[(t^{-1}-G)-\Delta]\right)\\ &=n_0(\varepsilon)-\frac{1}{\pi}\,\mathrm{Im\ Tr}\left(\tau^{\mathrm{U}}\frac{\partial}{\partial\varepsilon}(t^{-1}-G)\right)-\frac{1}{\pi}\,\mathrm{Im\ Tr}\frac{\partial}{\partial\varepsilon}\ln(1-\Delta\tau^{\mathrm{U}}).\end{aligned} \tag{A.11}$$

In equation (A.11), the first and second terms are just the DOS for the unperturbed system and the third term is the deviation from it due to the impurities, $\Delta n(\varepsilon)$. From the matrix identity $\mathrm{Tr}\ln A=\ln\det A$, $\Delta n(\varepsilon)$ can be written as

$$\Delta n(\varepsilon)=-\frac{1}{\pi}\,\mathrm{Im}\frac{\partial}{\partial\varepsilon}\ln\det(1-\Delta\tau^{\mathrm{U}}). \tag{A.12}$$

For example, $\Delta n_\alpha(\varepsilon)$ for a single impurity case, t_α at the origin, and $\Delta n_{\alpha\beta}(\varepsilon)$ for a two-impurity case, t_α at the origin and t_β at $\boldsymbol{R}_n$, are given by

$$\Delta n_\alpha(\varepsilon)=-\frac{1}{\pi}\,\mathrm{Im}\frac{\partial}{\partial\varepsilon}\ln\det[1-(t_0^{-1}-t_\alpha^{-1})(\tau^{\mathrm{U}})^{00}] \tag{A.13}$$

and

$$\Delta n_{\alpha\beta}(\varepsilon)=-\frac{1}{\pi}\,\mathrm{Im}\frac{\partial}{\partial\varepsilon}\ln\det\begin{bmatrix}1-(t_0^{-1}-t_\alpha^{-1})(\tau^{\mathrm{U}})^{00} & -(t_0^{-1}-t_\alpha^{-1})(\tau^{\mathrm{U}})^{0n}\\ -(t_0^{-1}-t_\beta^{-1})(\tau^{\mathrm{U}})^{n0} & 1-(t_0^{-1}-t_\beta^{-1})(\tau^{\mathrm{U}})^{nn}\end{bmatrix} \tag{A.14}$$

respectively.

Let us move to the derivation of equation (21). The total energy of a system including

two impurities α and β, $E_{\alpha\beta}$, is divided into the energy for the unperturbed system, E_U, the energy changes introduced independently by each impurity, $E_\alpha - E_U$ and $E_\beta - E_U$, and the interaction energy between the two impurities, $\Delta E_{\alpha\beta}$:

$$E_{\alpha\beta} = E_U + (E_\alpha - E_U) + (E_\beta - E_U) + \Delta E_{\alpha\beta}. \tag{A.15}$$

Then

$$\Delta E_{\alpha\beta} = \delta E_{\alpha\beta} - \delta E_\alpha - \delta E_\beta \tag{A.16}$$

with

$$\delta E_i = E_i - E_U \qquad i = \alpha, \beta \text{ or } \alpha\beta. \tag{A.17}$$

In the present problem, the double-counting Coulomb energy is expected to almost cancel on the right-hand side of equation (A.16). This is based on the following observations. (i) t_α and t_β are fixed quantities, irrespective of the configuration of the two impurities, in the single-site CPA calculation; (ii) the medium and the impurities are all iron and they differ only in the direction of the atomic magnetic moments, so that the charge disturbance in the medium induced by impurities may be very small. Therefore the net contribution of δE_i to $\Delta E_{\alpha\beta}$ comes from its band energy term:

$$\delta E_i = \sum_\sigma \int^{\varepsilon_F} d\varepsilon (\varepsilon - \varepsilon_F) \Delta n_i^\sigma(\varepsilon) \tag{A.18}$$

where $\Delta n_i^\sigma(\varepsilon)$ is the deviation of the DOS for the σ spin electron due to the impurity. By substituting equation (A.18) into equation (A.16) and using equations (A.13) and (A.14), we get

$$\Delta E_{\alpha\beta} = \frac{1}{\pi} \sum_\sigma \int^{\varepsilon_F} d\varepsilon \, \mathrm{Im} \ln \det(1 - K^{\alpha,\sigma}(\tau^c)^{0n} K^{\beta,\sigma}(\tau^c)^{n0}) \tag{A.19}$$

with

$$K^{\alpha,\sigma} = [1 - (t_c^{-1} - t_\alpha^{\sigma-1})(\tau^c)^{00}]^{-1}(t_c^{-1} - t_\alpha^{\sigma-1}) \tag{A.20}$$

where t_c and τ^c are the coherent single-site t matrix and the scattering path operator of the effective medium.

If the two impurity moments are parallel

$$\Delta E_P = \frac{1}{\pi} \sum_{\alpha=+,-} \int^{\varepsilon_F} d\varepsilon \, \mathrm{Im} \ln \det(1 - K^\alpha(\tau^c)^{0n} K^\alpha(\tau^c)^{n0}). \tag{A.21}$$

From the CPA condition given by equation (19), we can obtain equation (21) for the parallel moments:

$$\Delta E_P = \frac{2}{\pi} \int^{\varepsilon_F} d\varepsilon \, \mathrm{Im} \ln \det(1 - K^\alpha(\tau^c)^{0n} K^\alpha(\tau^c)^{n0}) \tag{A.22}$$

with $\alpha = +$ or $-$. If the two moments are antiparallel, we can obtain

$$\Delta E_{AP} = \frac{1}{\pi} \sum_{\substack{\alpha,\beta=+,- \\ (\alpha\neq\beta)}} \int^{\varepsilon_F} d\varepsilon \, \mathrm{Im} \ln \det(1 - K^\alpha(\tau^c)^{0n} K^\beta(\tau^c)^{n0}) \tag{A.23}$$

$$\Delta E_{AP} = \frac{2}{\pi} \int^{\varepsilon_F} d\varepsilon \, \mathrm{Im} \ln \det(1 + K^\alpha(\tau^c)^{0n} K^\alpha(\tau^c)^{n0}). \tag{A.24}$$

Appendix 2. Decoupling of four-spin correlation function

Collins and Marshall (1967) gave expressions for moments of the relaxation shape function $F(\boldsymbol{q}, \omega)$ in terms of the correlation function. In the expression for $\langle \omega^4 \rangle$, four-spin correlation functions appear which are decoupled into two-spin correlation functions. Equation (5.6) of Lovesey and Meserve (1973) is derived from the following decoupling scheme:

$$\langle S_i^x S_j^x S_k^z S_l^z \rangle \simeq \langle S_i^x S_j^x \rangle \langle S_k^z S_l^z \rangle \tag{A.25}$$

and

$$\langle S_i^z S_j^z S_k^z S_l^z \rangle \simeq \langle S_i^z S_j^z \rangle \langle S_k^z S_l^z \rangle + \langle S_i^z S_k^z \rangle \langle S_j^z S_l^z \rangle + \langle S_i^z S_l^z \rangle \langle S_j^z S_k^z \rangle. \tag{A.26}$$

We adopted a different decoupling scheme from equation (A.26) if at least two of i, j, k and l denote the same site. By using the identity

$$(S^z)^2 = S(S+1) - S^- S^+ - S^z \tag{A.27}$$

we derived the following equations:

$$\langle S_i^z S_i^z S_j^z S_j^z \rangle \simeq \tfrac{1}{9} S^2 (S+1)^2 - \langle S_i^z S_j^z \rangle \tag{A.28}$$

$$\langle S_i^z S_i^z S_j^z S_k^z \rangle \simeq \tfrac{1}{3} S(S+1) \langle S_j^z S_k^z \rangle \tag{A.29}$$

$$\langle S_i^z S_i^z S_i^z S_j^z \rangle \simeq \tfrac{1}{3} S(S+1) \langle S_i^z S_j^z \rangle. \tag{A.30}$$

In equations (A.28)–(A.30) it is assumed that i, j and k are mutually different. The use of this decoupling scheme slightly sharpens the peak in $S(\boldsymbol{q}, \omega)$ for the constant-ω plot compared with the use of equation (A.26) for all combinations of i, j, k and l.

References

Bansil A 1975 *Solid State Commun.* **16** 885–9

von Barth U and Hedin L 1972 *J. Phys. C: Solid State Phys.* **5** 1629–42

Bieber A, Gautier F, Treglia G and Ducastelle F 1981 *Solid State Commun.* **39** 149–53

Callaway J and Wang C S 1977 *Phys. Rev.* B **16** 2095–105

Collins M F and Marshall W 1967 *Proc. Phys. Soc.* **92** 390–9

Edwards D M 1981 *Electron Correlation and Magnetism in Narrow Band Systems* ed. T Moriya (Berlin: Springer) pp 73–83

Gunnarsson O and Lundqvist B I 1976 *Phys. Rev.* B **13** 4274–98

Gyorffy B L and Stocks G M 1979 *Electrons in Disordered Metals and at Metalic Surfaces* ed. P Phariseau, B L Gyorffy and L Scheire (New York: Plenum) pp 89–192

Hasegawa H 1979 *J. Phys. Soc. Japan* **46** 1504–14

—— 1980 *J. Phys. Soc. Japan* **49** 963–71

—— 1981 *Electron Correlation and Magnetism in Narrow Band Systems* ed. T Moriya (Berlin: Springer) pp 38–50

Holden A J and You M V 1982 *J. Phys. F: Met. Phys.* **12** 195–214

Hubbard J 1979a *Phys. Rev.* B **19** 2626–36

—— 1979b *Phys. Rev.* B **20** 4584–95

—— 1981 *Phys. Rev.* B **23** 5974–7

Inoue M and Moriya T 1967 *Prog. Theor. Phys.* **38** 41–60

Kakehashi Y 1981a *J. Phys. Soc. Japan* **50** 1505–12

—— 1981b *J. Phys. Soc. Japan* **50** 1925–33

Lacour-Gayet P and Cyrot M 1974 *J. Phys. C: Solid State Phys.* **7** 400–8

Lin-Chung P J and Holden A J 1981 *Phys. Rev.* B **23** 3414–20
Lovesey S W and Meserve R A 1973 *J. Phys. C: Solid State Phys.* **6** 79–97
Lynn J W 1975 *Phys. Rev.* B **11** 2624–37
Moriya T 1982 *J. Phys. Soc. Japan* **51** 2806–18
Moriya T and Hasegawa H 1980 *J. Phys. Soc. Japan* **48** 1490–503
Moriya T and Takahashi Y 1978 *J. Phys. Soc. Japan* **45** 397–408
Moruzzi V L, Janak J F and Williams A R 1978 *Calculated Electronic Properties of Metals* (Oxford: Pergamon)
Nakagawa Y 1956 *J. Phys. Soc. Japan* **8** 855–63
Nix F C and MacNair D 1941 *Phys. Rev.* **60** 597–605
Petersson L G, Melander R, Spears D P and Hagstrom B M 1976 *Phys. Rev.* B **14** 4177–83
Prange R E 1981 *Electron Correlation and Magnetism in Narrow Band Systems* ed. T Moriya (Berlin: Springer) pp 55–72
Prange R E and Korenman V 1979a *Phys. Rev.* B **19** 4691–7
—— 1979b *Phys. Rev.* B **19** 4698–702
Shastry B S, Edwards D M and Young A P 1981 *J. Phys. C: Solid State Phys.* **14** 1665–70
Temmerman W M 1982 *J. Phys. F: Met. Phys.* **12** 125–9
Terakura K, Hamada N, Oguchi T and Asada T 1982 *J. Phys. F: Met. Phys.* **12** 1661–78
Wang C S, Prange R E and Korenman V 1982 *Phys. Rev.* B **25** 5766–77
You M V and Heine V 1982 *J. Phys. F: Met. Phys.* **12** 177–94